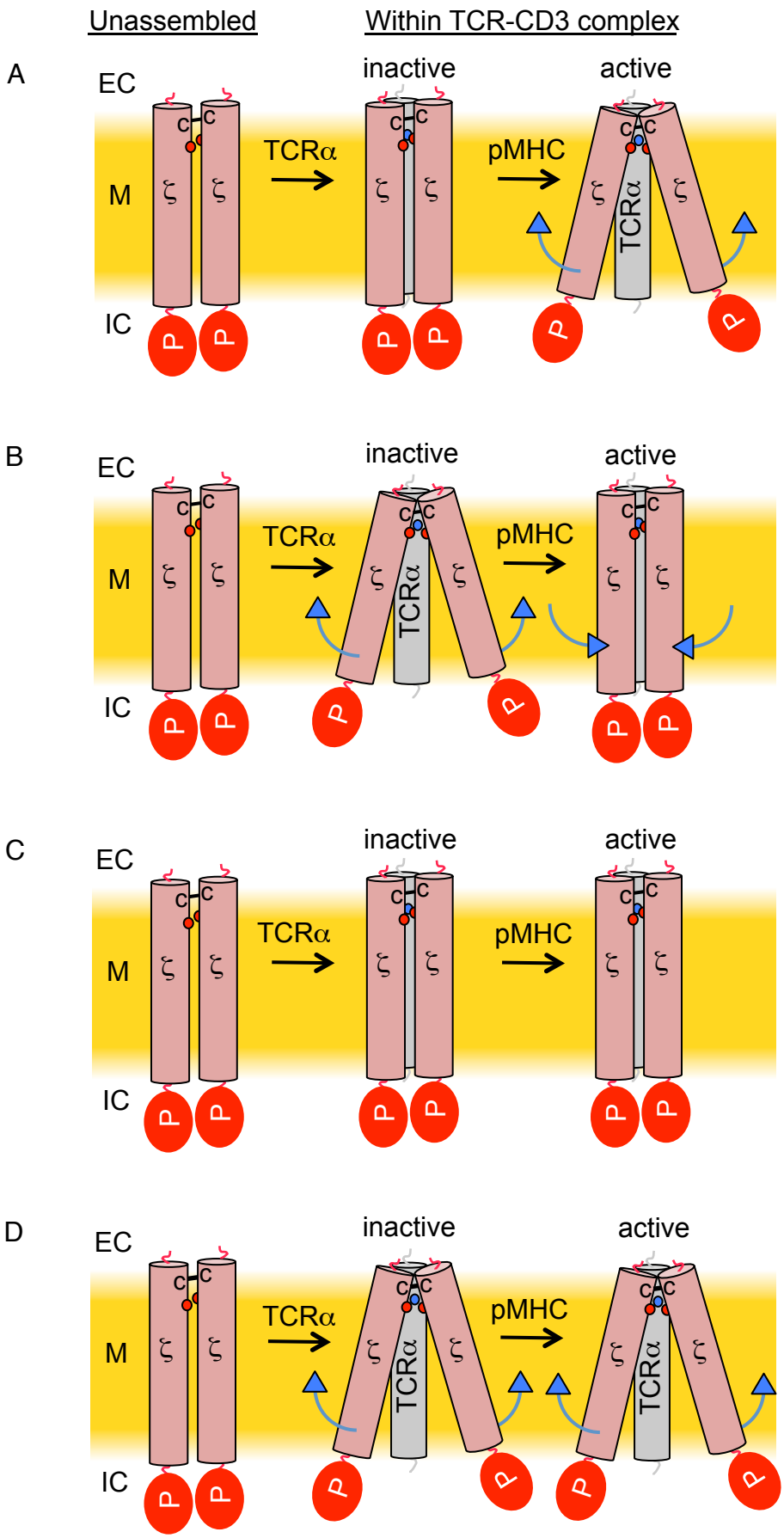
Unassembled
Within TCR-CD3 complex
A
B
C
D
EC
M
IC
inactive
active
TCRα
pMHC
ζ
C
P

Figure S1

Figure S1. Possible experimental outcomes of the tested hypothesis, related to text and Experimental Procedures.

The CD3ζζ TMDs (red cylinder) and the associated TCRα TMD (grey cylinder) are illustrated with the cysteines (c—c) that mediate the intra-chain disulfide bond and the charged residues that mediate interactions between the TCRα (blue dot = arginine) and CD3ζζ (red dots = aspartate) TMDs. The extracellular (EC), intramembrane (M = yellow) and intracellular (IC) space are shown for reference regarding where the TMDs emerge into the cytoplasm (i.e. the cytoplasmic juxtamembrane region). The CD3ζζ TMDs in the unassembled state are illustrated based on the NMR structure (PDB 2HAC) (Call et al., 2006). All possible outcomes are predicated on this structure as it serves as the experimental reference point for changes in the subunits upon assembly within a TCR-CD3 complex and upon TCR engagement.

(**A and B**) Models for the relay of pMHC-specific information across the cell membrane that are consistent with the tested hypothesis. Models consistent with triggering mechanism in which the CD3ζζ subunits (**A**) emerge from the membrane together within an unengaged TCR-CD3 complex and are divaricated upon TCR engagement or (**B**) emerge from the membrane apart within an unengaged TCR-CD3 complex and are juxtaposed upon TCR engagement.

(**C and D**) Models that are inconsistent with the tested hypothesis because the spatial relationship between the cytosolic juxtamembrane regions of the CD3ζζ subunits do not change within a TCR-CD3 complex upon TCR engagement.

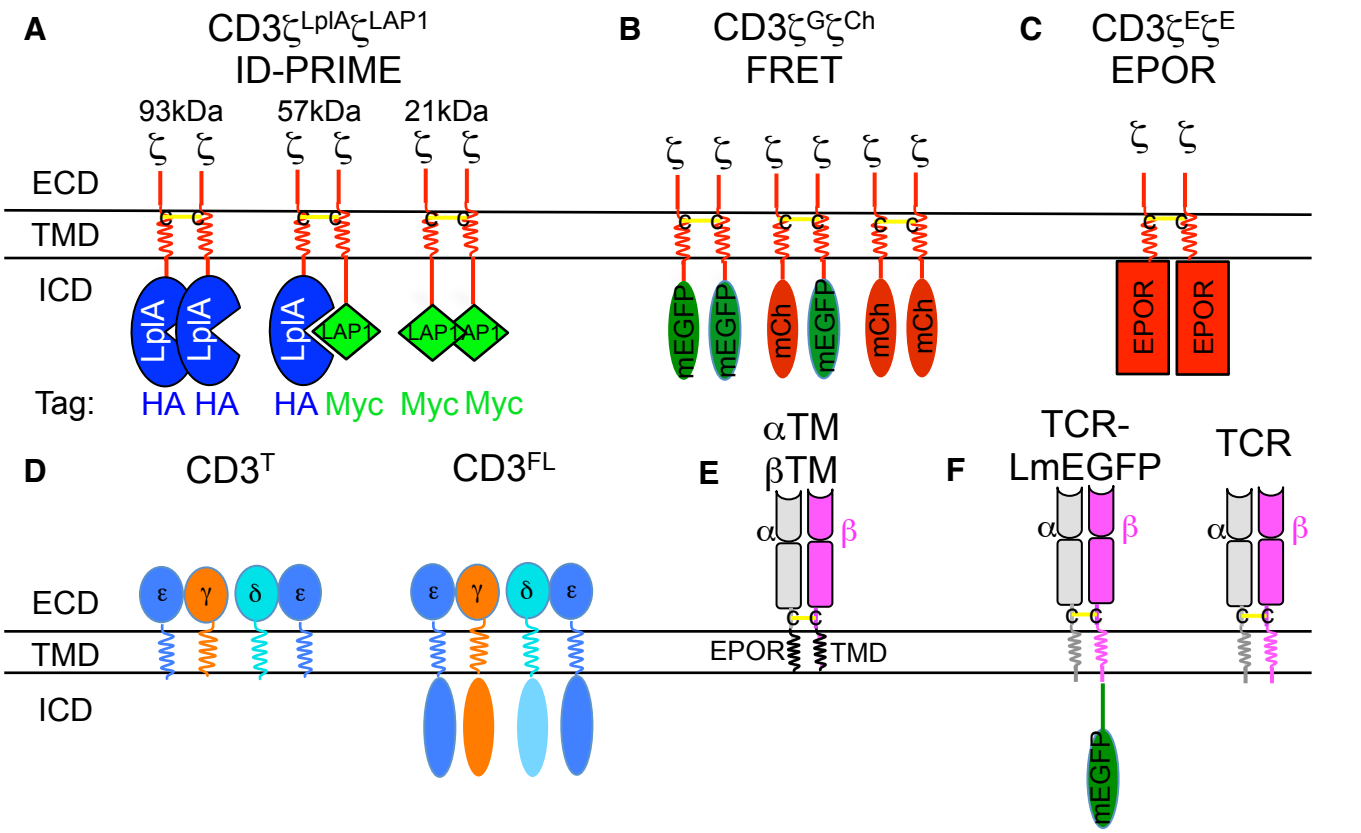
A
CD3ζ^LplAζ^LAP1
ID-PRIME
93kDa
57kDa
21kDa
ECD
TMD
ICD
LplA
LAP1
Tag:
HA HA
HA Myc
Myc Myc
B
CD3ζ^GζCh
FRET
mEGFP
mCh
C
CD3ζ^EζE
EPOR
D
CD3^T
CD3^FL
ε
γ
δ
E
αTM
βTM
EPOR
TMD
F
TCR-
LmEGFP
TCR

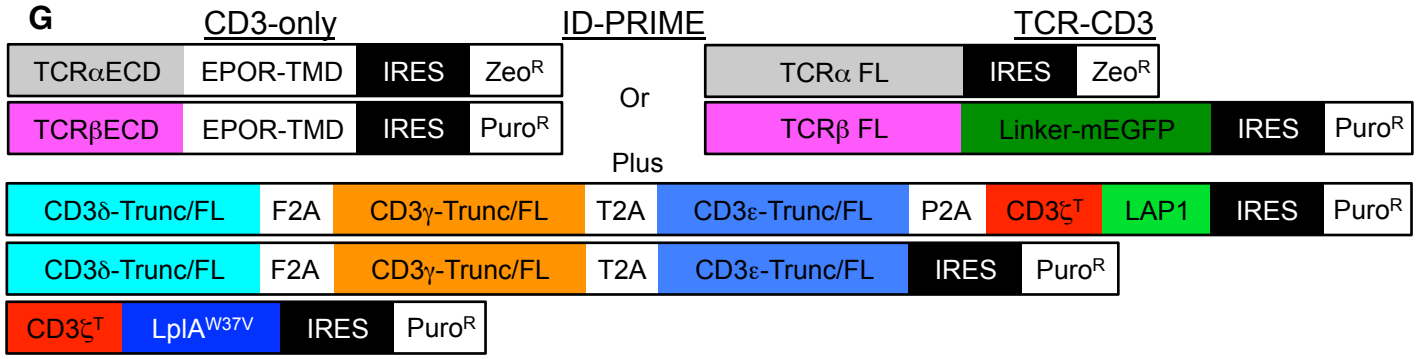
G
CD3-only
ID-PRIME
TCR-CD3
TCRαECD
EPOR-TMD
IRES
Zeo^R
TCRβECD
Puro^R
Or
TCRα FL
TCRβ FL
Linker-mEGFP
Plus
CD3δ-Trunc/FL
F2A
CD3γ-Trunc/FL
T2A
CD3ε-Trunc/FL
P2A
CD3ζ^T
LAP1
CD3ζ^T
LplA^W37V

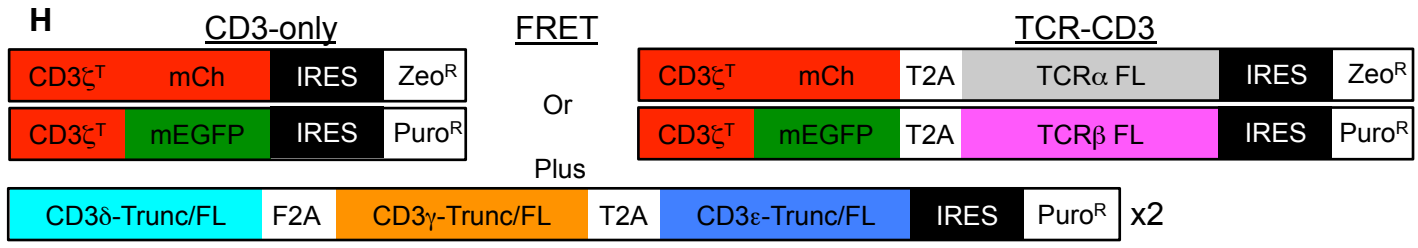
H
CD3-only
FRET
TCR-CD3
CD3ζ^T
mCh
IRES
Zeo^R
mEGFP
Puro^R
Or
T2A
TCRα FL
TCRβ FL
Plus
CD3δ-Trunc/FL
F2A
CD3γ-Trunc/FL
CD3ε-Trunc/FL
x2

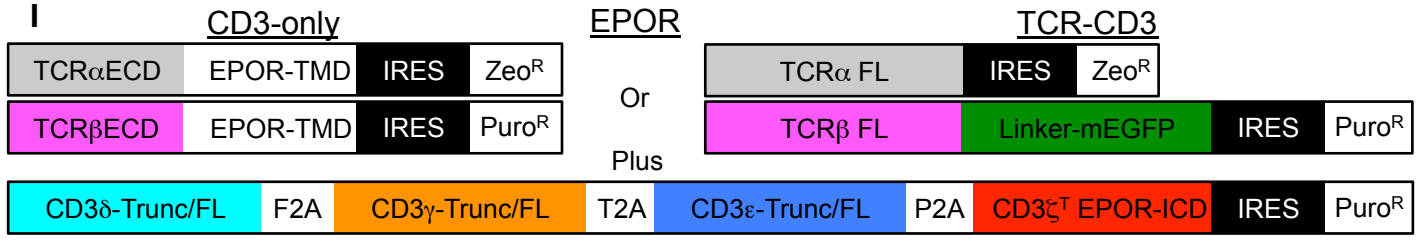
I
CD3-only
EPOR
TCR-CD3
TCRαECD
EPOR-TMD
IRES
Zeo^R
TCRβECD
Puro^R
Or
TCRα FL
TCRβ FL
Linker-mEGFP
Plus
CD3δ-Trunc/FL
F2A
CD3γ-Trunc/FL
T2A
CD3ε-Trunc/FL
P2A
CD3ζ^T EPOR-ICD

Figure S2

Figure S2. Engineered TCR-CD3 complex subunits and constructs used in this study, related to Experimental Procedures and Supplementary Experimental Procedures.
(**A-F**) Shown are illustrations of the CD3ζ chimeras, truncated or full-length CD3 subunits (CD3$\gamma^{T/FL}$, $\delta^{T/FL}$, and $\varepsilon^{T/FL}$), and non-assembling filler TCR (lacking TMD charged residues) or full-length assembling TCR subunits. M12 cell were used for the ID-PRIME and FRET systems. Ba/F3 cells were used for the EPOR system. The linker lengths between CD3ζ^{T} and the proximity probes are indicated under constructs in the Supplementary Experimental Procedures.
(**A**) CD3ζ-LplA^{W37V} (CD3ζ^{LplA}) and CD3ζ-LAP1 (CD3ζ^{LAP1}).
(**B**) CD3ζ-mEGFP (CD3ζ^{G}) and CD3ζ-mCherry (CD3ζ^{Ch}).
(**C**) CD3ζ-EPOR (CD3ζ^{E}) chimeras.
(**D**) CD3γ^{T}, CD3δ^{T}, and CD3ε^{T} lacking their ICDs and wild-type CD3γ^{FL}, CD3δ^{FL}, and CD3ε^{FL}.
(**E**) αTM (TCRα ECD + EPOR TMD) and βTM (TCRβ ECD + EPOR TMD). These make a surface heterodimer that lack the TMD charge residues that are essential for complex assembly (Call et al., 2002; Kuhns et al., 2010). The were used as "space-fillers" in the ID-PRIME and EPOR systems, as illustrated below and described in experimental procedures, so that each CD3-only cell line was transduced with the same number of constructs with the same drug resistance. Surface expression could be monitored by flow cytometry as previously reported (Kuhns et al., 2010).
(**F**) TCR-LmEGFP (TCRα + TCRβ fused to mEGFP via a long linker) and TCR (TCRα + TCRβ) were used in TCR-CD3 cells for full complex assembly.
(**G-I**) Shown are schematics of the coding regions for the retroviral constructs used to generate CD3-only and TCR-CD3 cells expressing truncated or full length CD3 subunits in the (**G**) ID-PRIME, (**H**) FRET, and (**I**) EPOR systems. The ID-PRIME and FRET lines were generated with two copies worth of CD3γ, CD3δ, and CD3ε to match the two copies of CD3ζ subunits.

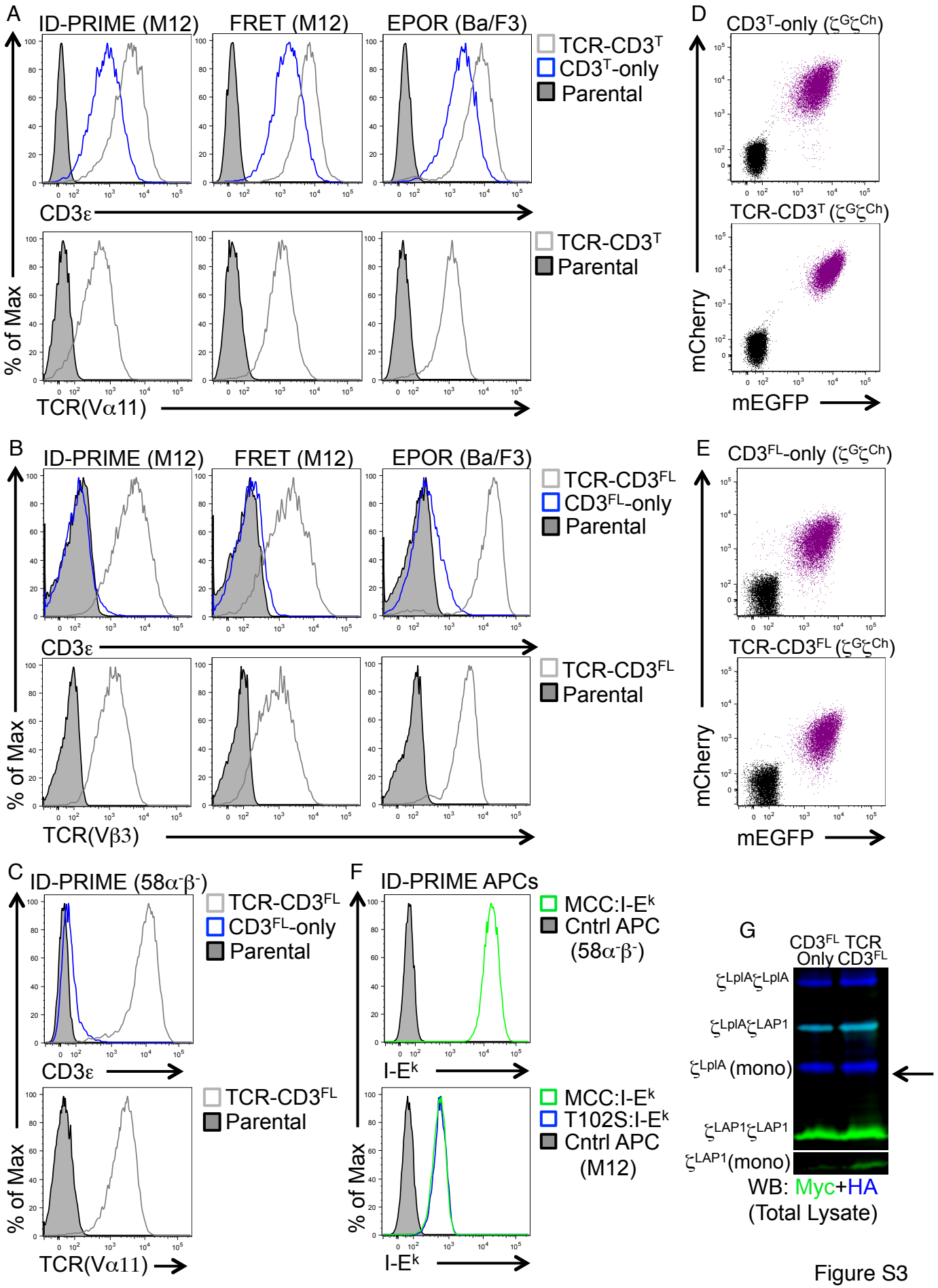
A
ID-PRIME (M12)
FRET (M12)
EPOR (Ba/F3)
TCR-CD3T
CD3T-only
Parental
CD3ε
% of Max
TCR(Vα11)
B
ID-PRIME (M12)
FRET (M12)
EPOR (Ba/F3)
TCR-CD3FL
CD3FL-only
Parental
CD3ε
% of Max
TCR(Vβ3)
C
ID-PRIME (58α-β-)
TCR-CD3FL
CD3FL-only
Parental
CD3ε
% of Max
TCR(Vα11)
F
ID-PRIME APCs
MCC:I-Ek
Cntrl APC
(58α-β-)
I-Ek
% of Max
MCC:I-Ek
T102S:I-Ek
Cntrl APC
(M12)
I-Ek
D
CD3T-only (ζGζCh)
TCR-CD3T (ζGζCh)
mCherry
mEGFP
E
CD3FL-only (ζGζCh)
TCR-CD3FL (ζGζCh)
mCherry
mEGFP
G
CD3FL TCR
Only CD3FL
ζLplAζLplA
ζLplAζLAP1
ζLplA (mono)
ζLAP1ζLAP1
ζLAP1(mono)
WB: Myc+HA
(Total Lysate)

Figure S3

Figure S3. Characterization of cell lines engineered for this study, related to Text, Experimental Procedures, Supplementary Experimental Procedures, and Figure S2.
(**A and B**) Flow cytometry analysis of CD3ε (top) and TCR expression (bottom, Vα11 or Vβ3) are shown for M12 or Ba/F3 cells in the ID-PRIME and FRET, or EPOR experimental systems, respectively, as labeled. (**A)** Cells expressing $CD3^{T}$ subunits. Truncated CD3ε is known to reach the cell surface on its own due to a lack of ER retention signals, but increases upon assembly into the TCR-$CD3^{T}$ complex due to increased surface half-life (not shown), while the TCR does not reach the cell surface without full complex assembly (Bonifacino et al., 1989; Delgado and Alarcon, 2005; Kuhns et al., 2010; Tan et al., 1991). (**B**) Full length CD3ε has minimal cell surface expression until assembled within a full TCR-$CD3^{FL}$ complex.
(**C**) Flow cytometry analysis of full length CD3ε (top) and TCR expression (bottom, Vα11) on $CD3^{FL}$-only and TCR-$CD3^{FL}$ $58\alpha^{-}\beta^{-}$ cells.
(**D and E**) Proportional expression of $CD3\zeta^{G}$ and $CD3\zeta^{Ch}$. Flow cytometry analysis of CD3-only and TCR-CD3 cells used in the FRET experiments for cells expressing (**D**) truncated CD3 subunits or (**E**) full-length CD3 subunits. Parental M12 cells (black) are shown in comparison with the experimental cells (purple) for $CD3\zeta^{G}$ (mEGFP) and $CD3\zeta^{Ch}$ (mCherry) expression as labeled. Diagonal indicates proportionality of expression.
(**F**) $I\text{-}E^{k}$ expression on engineered APCs. (Top) MCC:$I\text{-}E^{k}$ expression on agonist pMHC or parental control $58\alpha^{-}\beta^{-}$ cells are shown. (Bottom) MCC:$I\text{-}E^{k}$ or T102S:$I\text{-}E^{k}$ expression on agonist pMHC or parental control M12 cells are shown.
(**G**) Absence of free LplA in $CD3^{FL}$-only and TCR-$CD3^{FL}$ cells. Whole cell lysates of $CD3^{FL}$-only and TCR-$CD3^{FL}$ $58\alpha^{-}\beta^{-}$ cells are shown and labeled as in **Figure 1B** to illustrate that the band running below the $CD3\zeta^{LplA}$ monomer in the $CD3^{T}$-only and TCR-$CD3^{T}$ cells was eliminated due to removal of a start codon in the fusion between CD3ζ and LplA. Arrow indicates where this free LplA ran in the previous cell lines.

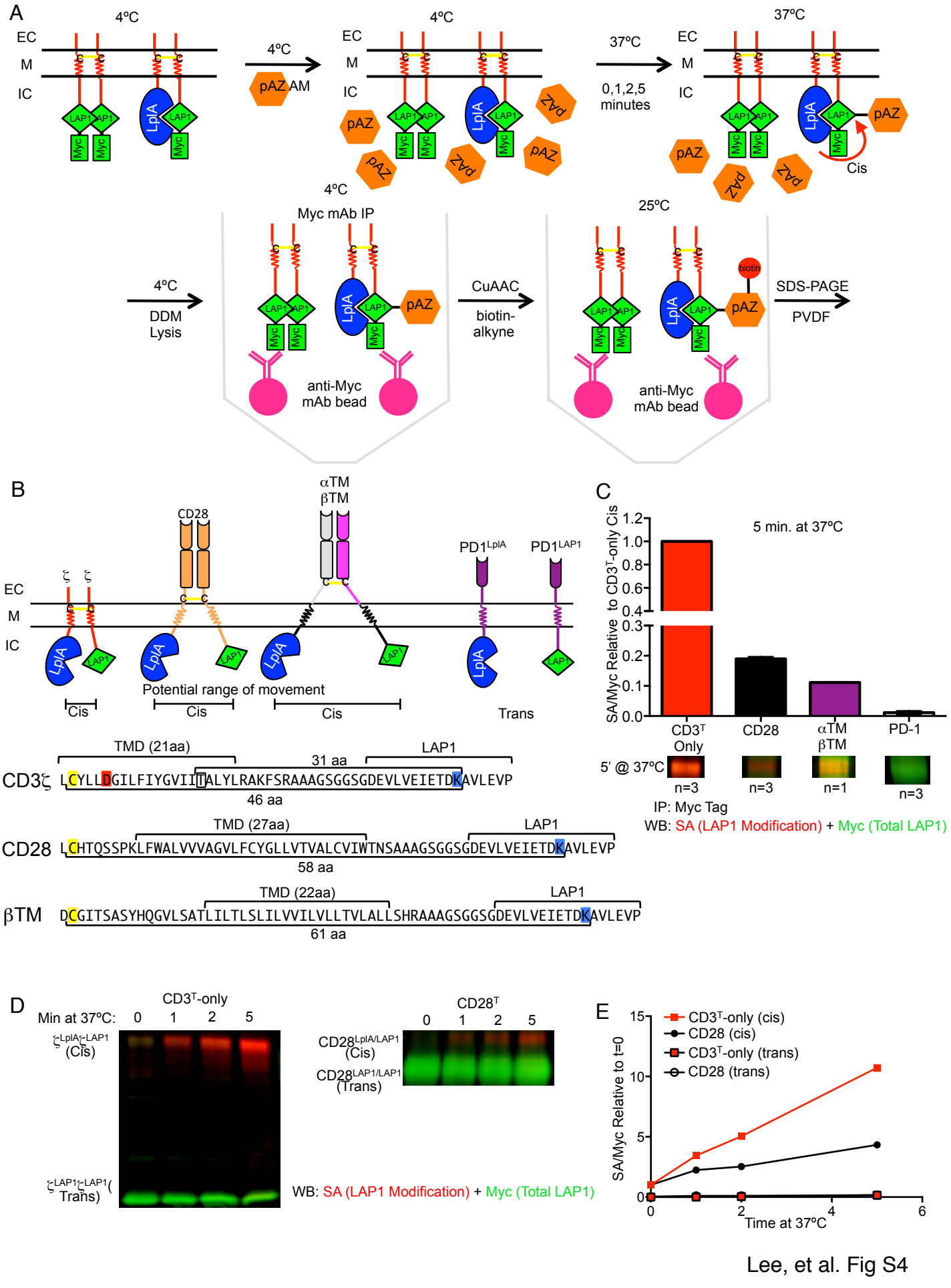

Lee, et al. Fig S4

Figure S4. ID-PRIME workflow and controls, related to Experimental Procedures, Text, and Figure 1.

(**A**) ID-PRIME workflow. Cells expressing CD3ζ^{LplA} (probe ligase) and CD3ζ^{LAP1} (peptide substrate) chimeras were chilled to 4ºC on ice, loaded with membrane permeant pAz (pAz-acetoxymethyl ester (AM)), then shifted to 37ºC to allow probe ligation. The reaction was halted at 4ºC. Cells were lysed in DDM and the CD3ζ^{LplA}ζ^{LAP1} and CD3ζ^{LAP1}ζ^{LAP1} peptide substrate chimeras were immunoprecipitated (IP) with anti-Myc beads. pAz was biotinylated by CuAAC at 25ºC prior to size separation by non-reducing SDS-PAGE and blotting for ligated LAP1 (streptavidin) versus total peptide substrate amounts (anti-myc).

(**B**) Cartoon and TMD-ICD sequence of control chimeric proteins used to assess intra-module cis interactions at the cytoplasmic juxtamembrane regions (JM) by ID-PRIME. The CD3ζ^{LplA}ζ^{LAP1} module is shown with a yellow N-terminal TMD disulfide bond (c = cysteine). Parallel TMD helices are depicted because the solution structure shows contacts at both the N- and C-termini (Call et al., 2006). The LplA and LAP1 regions are shown spreading apart on their short flexible linkers to illustrate the potential range of movement that the ligase and substrate could achieve at steady state for unassembled modules in CD3-only cells (not drawn to scale). This would impact the local concentration and rate of ID-PRIME. The CD3ζ sequence shows the TMD-ICD sequence labeled with the TMD and LAP1 sequences bracketed. The intracellular cysteine is shaded yellow and the lysine that interacts with TCRα is blue. The C-terminal threonine that mediates intra-module TMD interactions is boxed (Call et al., 2006). The bracket from this residue to the blue lysine indicates the length of sequence that could allow mobility for an unassembled CD3ζ^{LplA}ζ^{LAP1} module. The CD28^{LplA}CD28^{LAP1} module is shown with the intra-chain disulfide bond and TMD-ICD sequence labeled or highlighted as above. An αTM^{LplA}βTM^{LAP1} module similar to **Figure S1E** is shown labeled and highlighted as above. For this module and CD28, the connecting peptide-TMD-ICD regions are shown to swing apart from the intra-chain disulfide to illustrate the potential range of movement. Finally, PD1^{LplA} and PD1^{LAP1} are shown in purple. Cells expressing these monomers served as a negative control.

(**C**) Cis interactions are proportional to the distance between the intra-chain interactions and the ligase and substrate. ID-PRIME was performed with M12 cells expressing the chimeras illustrated in (**B**) for 5 minutes at 37ºC. LAP1 modification of the cis species relative to LAP1 levels (SA/Myc) are shown normalized to the CD3-only sample. Inset bands from one experiment on the same gel are shown as labeled (n = number of experiments with one replicate per experiment).

(**D**) CD3ζζ JM cis interactions occur more rapidly than those for CD28. Kinetic analysis of CD3ζζ and CD28 JM cis interactions by ID-PRIME were performed as in **Figure 1D** simultaneously. Represents side-by-side one kinetic experiment. Samples were cropped from the same gel for presentation and comparison due to mobility differences.

(**E**) LAP1 modification (SA) is shown relative to total LAP1 (anti-myc) normalized to the zero time point signal for both cis and trans species as labeled for the blots in (**D**).

A

$F^c = F^b - [(F_d^b/D_d^b) \times D^b] - [(F_a^b/A_a^b) \times A^b]$

F^c = Corrected FRET (FRETc)

F^b = Observed FRET (background corrected)

F_d^b/D_d^b= Donor bleed through correction factor FRET channel/Donor channel intensity for

D^b = Donor (mEGFP) intensity (background corrected)

A^b = Acceptor (mCh) intensity (background corrected)

F_a^b/A_a^b= Acceptor bleed through correction factor FRET channel/Acceptor channel intensity for single color acceptor (background corrected)

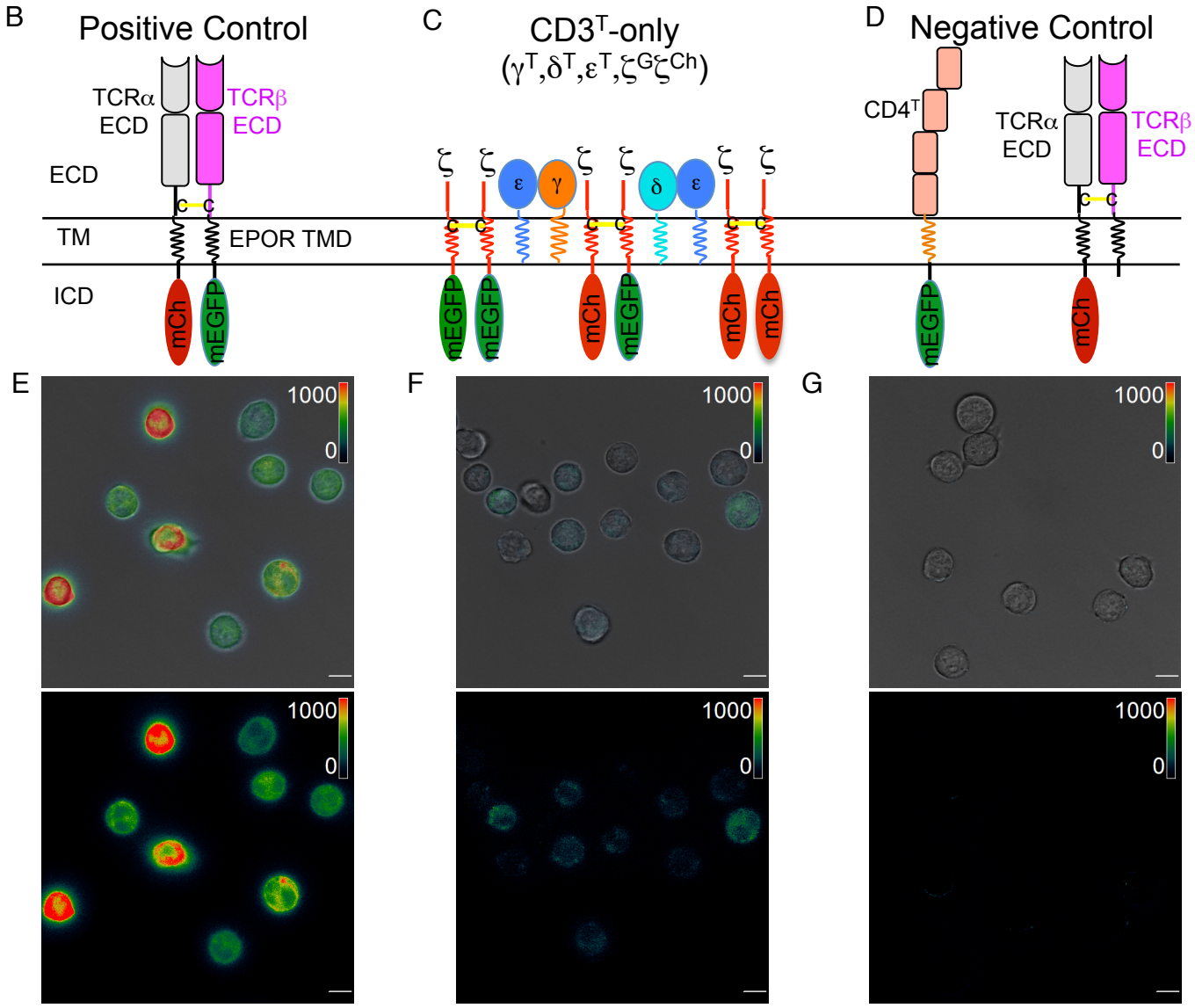

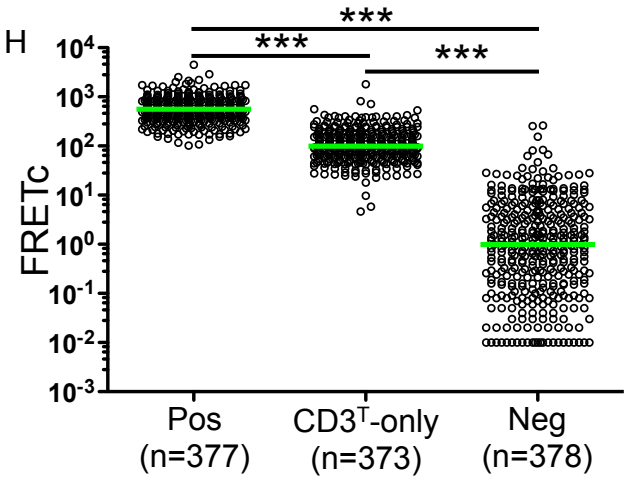

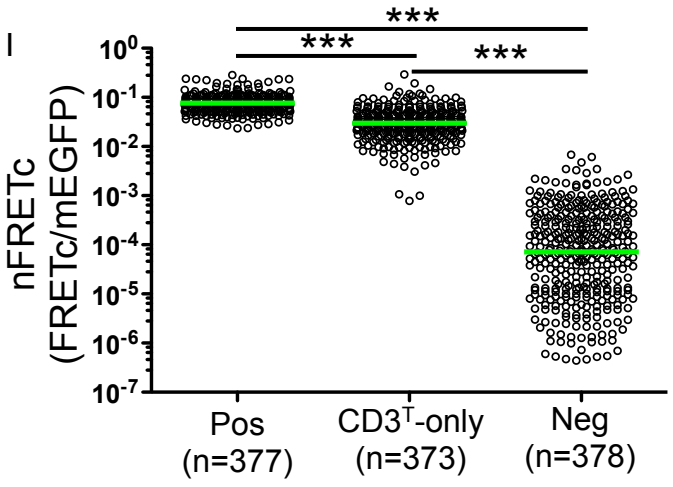

Figure S5

Figure S5. FRETc analysis, related to Figures 2.

(**A**) Formula for deriving FRETc values from three-channel sensitized emission data (Youvan et al., 1997) used in the SlideBook software FRET module (3I).

(**B-D**) Control mEGFP and mCherry chimeras. (**B**) Positive control chimeras. TCRα and TCRβ ectodomains were fused to the transmembrane domain of EPOR (to allow cell surface expression without the CD3 subunits) and mCherry (TCRαTM-mCh) or mEGFP (TCRβTM-mEGFP) via a minimal linker (~17Å). (**C**) The CD3 subunits are shown for comparison. (**D**) C-terminally truncated CD4 was fused to mEGFP via the short linker ($CD4^{T}$-mEGFP) and co-expressed with TCRαTM-mCh plus TCRβTM in M12 cells as a negative control.

(**E-G**) Wide field FRET images. Pseudocolored FRETc values are shown overlaid on bright field images (top) or broken out on their own (bottom) at 60X. The scale bar is 10μm. The CD3-only pseudocolor images shown here scaled from 0-1000 is the same image shown in **Figure 2** scaled from 0-500.

(**H and I**) Significant differences in (**H**) FRETc and (**I**) nFRETc values were observed in positive control, CD3-only, and negative control M12 cells. Each dot represents a single cell, the green line represents the median population value, and the data are concatenated data from two populations imaged on separate days (~200 cells/population; ***$p<0.0001$ Kruskal-Wallis ANOVA and Dunn's Post Test for non-parametric data).

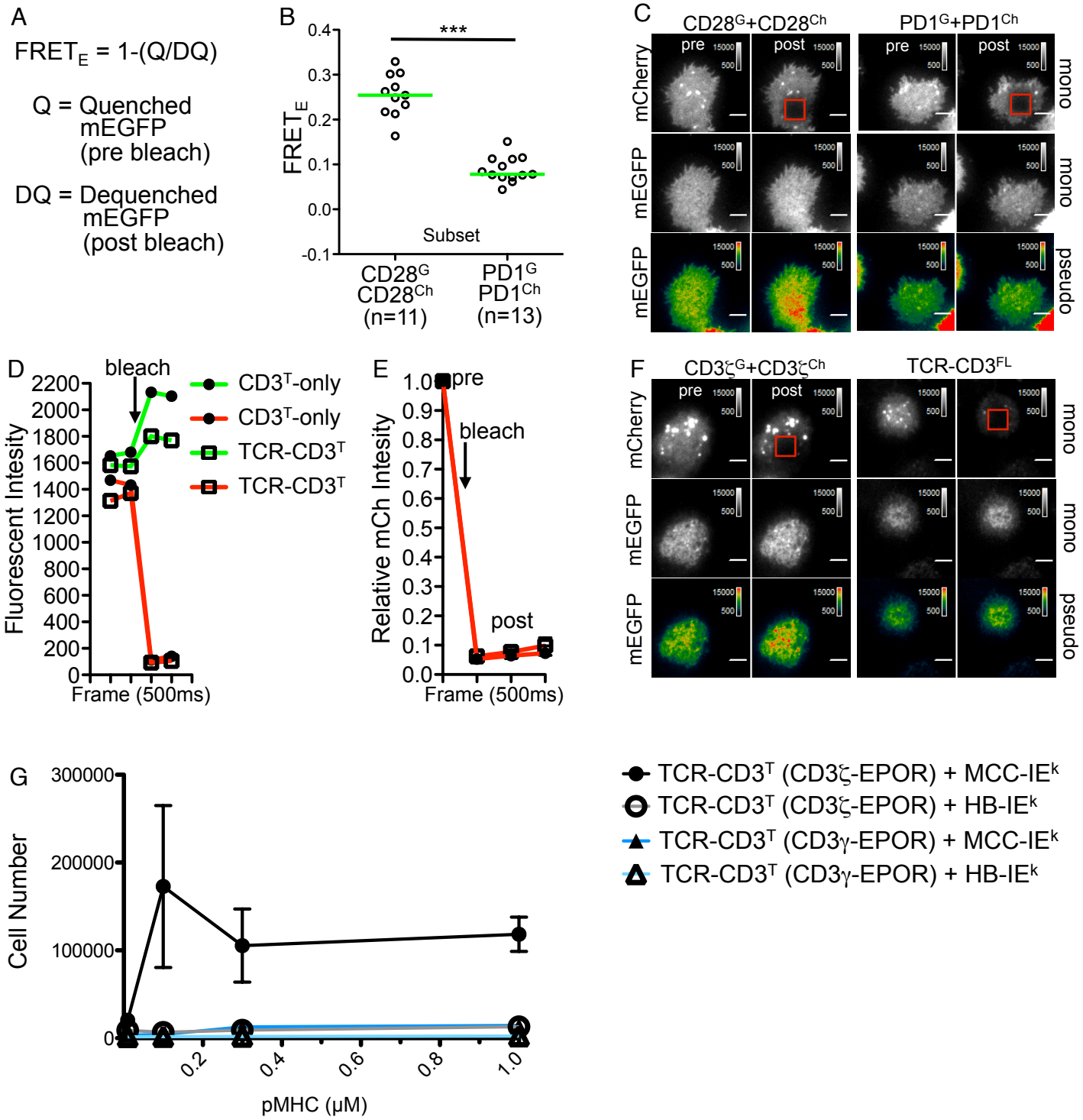
A
FRET_E = 1-(Q/DQ)
Q = Quenched mEGFP (pre bleach)
DQ = Dequenched mEGFP (post bleach)
B
***
FRET_E
Subset
CD28^G CD28^Ch (n=11)
PD1^G PD1^Ch (n=13)
C
CD28^G+CD28^Ch
PD1^G+PD1^Ch
pre
post
mCherry
mEGFP
mono
pseudo
D
bleach
CD3^T-only
CD3^T-only
TCR-CD3^T
TCR-CD3^T
Fluorescent Intesity
Frame (500ms)
E
pre
bleach
post
Relative mCh Intesity
Frame (500ms)
F
CD3ζ^G+CD3ζ^Ch
TCR-CD3^FL
G
Cell Number
pMHC (μM)
TCR-CD3^T (CD3ζ-EPOR) + MCC-IE^k
TCR-CD3^T (CD3ζ-EPOR) + HB-IE^k
TCR-CD3^T (CD3γ-EPOR) + MCC-IE^k
TCR-CD3^T (CD3γ-EPOR) + HB-IE^k

Figure S6

Figure S6. $FRET_E$ and EPOR analysis of conformational changes, related to Text and Figure 3.

(**A-F**) Donor recovery after photobleaching.

(**A**) The formula for deriving $FRET_E$ values (Xu et al., 2008).

(**B**) $FRET_E$ as measured by TIRFM is shown for subsets of M12 cells expressing C-terminally truncated versions of CD28 (independent positive control) or PD-1 (negative control) fused to mEGFP or mCh via short linkers. CD28 is a disulfide-bonded heterodimer like CD3ζζ so these cells should express $CD28^{G}CD28^{G}$, $CD28^{G}CD28^{Ch}$, and $CD28^{Ch}CD28^{Ch}$ species and were expected to FRET. PD-1 is a monomer and was not expected to FRET. Cells were cultured for 10 minutes at 37ºC on coverslips prior to imaging. Bright mCherry vesicles were observed in both cells, as in the CD3-only and TCR-CD3 cells, but were not observed to impact FRET. Note that CD28 and PD-1 expression was brighter for mEGFP and mCherry than the CD3-only and TCR-CD3 cells and the ROI fill in more quickly (not shown), but subset analysis was performed based on the same criteria (see Supplemental Experimental Procedures). Dots represent single cells and green bars represent median values (***$p<0.0001$; Mann-Whitney).

(**C**) $FRET_E$ is higher in positive control (CD28) cells than negative control (PD-1) cells. TIRFM images pre and post mCherry bleaching. mCherry is shown in grey scale. mEGFP is shown in grey scale and pseudocolor. Scale bar is 5μm.

(**D**) Differences in donor recovery between $CD3^{T}$-only and TCR-$CD3^{T}$ cells after acceptor ablation. mEGFP (green) and mCherry (red) intensity levels are shown for two exposures prior to bleaching mCherry and two exposures post bleaching for the $CD3^{T}$-only and TCR-$CD3^{T}$ cells shown in **Figure 3A**.

(**E**) Acceptor photobleaching at the population level. mCherry (red) levels are shown for one acquisition pre-photobleaching and three acquisition frames post-photobleaching for the $CD3^{T}$-only (closed circles) and TCR-$CD3^{T}$ populations (open squares) shown in **Figure 3B**. Equivalent recovery of $CD3\zeta^{Ch}$ molecules was observed in both populations, so any influence of diffusing molecules on $FRET_E$ calculations are equivalent.

(**F**) FRET is lower in TCR-$CD3^{FL}$ cells at the membrane. TIRFM images pre and post mCherry bleaching. mCherry is shown in grey scale. mEGFP is shown in grey scale and pseudocolor. Scale bar is 5μm. Representative images for data in **Figure 3C**.

(**G**) TCR-driven proliferation of Ba/F3 cells expressing TCR-$CD3^{T}$ complexes with CD3ζ-EPOR chimeras. Ba/F3 cells expressing TCR-$CD3^{T}$ complexes including either CD3ζ-EPOR or CD3γ-EPOR chimeras (Kuhns, et al., 2010) were cultured on glass surfaces coated with solutions containing the indicated concentrations of agonist pMHC (MCC-IE^{k}) or null pMHC (HB-IE^{k}). Proliferation after 3 days culture was enumerated by flow cytometry (mean +/-SEM). The surfaces were prepared by the same protocol used for imaging. These data are from one of three similar experiments performed with a single cell line. The magnitude of proliferation was variable between experiments, with this being the most robust we observed.

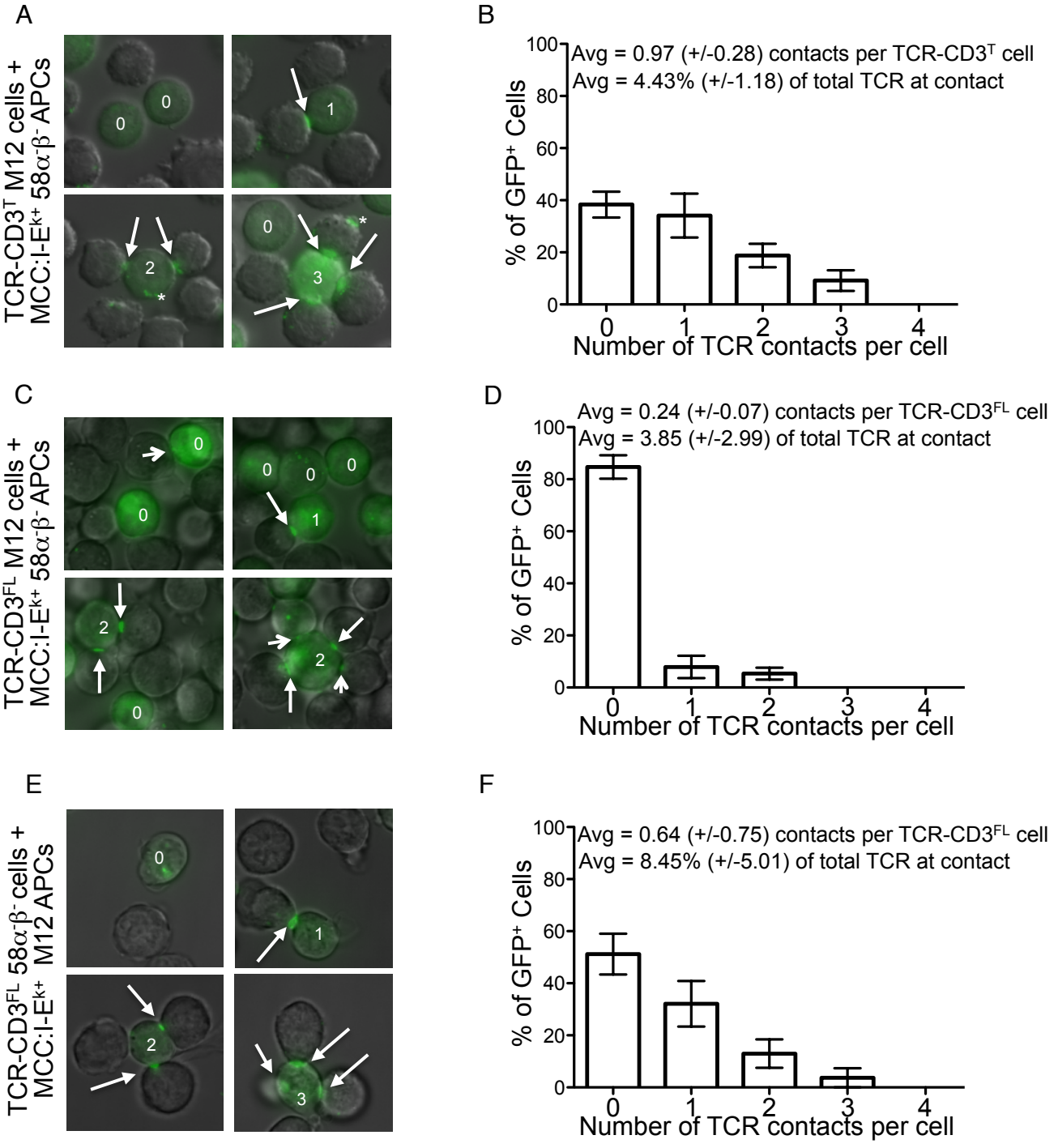
A
TCR-CD3T M12 cells + MCC:I-Ek+ 58α-β- APCs
B
Avg = 0.97 (+/-0.28) contacts per TCR-CD3T cell
Avg = 4.43% (+/-1.18) of total TCR at contact
% of GFP+ Cells
Number of TCR contacts per cell
C
TCR-CD3FL M12 cells + MCC:I-Ek+ 58α-β- APCs
D
Avg = 0.24 (+/-0.07) contacts per TCR-CD3FL cell
Avg = 3.85 (+/-2.99) of total TCR at contact
% of GFP+ Cells
Number of TCR contacts per cell
E
TCR-CD3FL 58α-β- cells + MCC:I-Ek+ M12 APCs
F
Avg = 0.64 (+/-0.75) contacts per TCR-CD3FL cell
Avg = 8.45% (+/-5.01) of total TCR at contact
% of GFP+ Cells
Number of TCR contacts per cell

Figure S7

Figure S7. Cell-cell interactions for ID-PRIME TCR engagement, related to Figures 6 and 7.

(**A-F**) Counting TCR-CD3 cell contacts with $pMHC^{+}$ APCs. (**A**) MCC:I-E^{k+} APCs ($58\alpha^{-}\beta^{-}$) were pelleted with TCR-$CD3^{T}$ M12 cells at a 5:1 ratio and incubated for five minutes at 37ºC prior to imaging. (**A**) Maximum projections of z-stacks (30, 1µm) for mEGFP and are shown overlaid with DIC. Arrows indicate cell-cell contacts with TCR accumulation. Asterisks mark TCR clusters not observed at a cell-cell interface that may have occurred during pellet disruption for imaging if couples were sheared apart. (**B**) The number of contacts per TCR-$CD3^{T}$ M12 cells are shown as a percent of the total cells analyzed (n=72). Bars represent the mean number of contacts per field of cells +/- SEM between fields. Insets indicate the average number of contacts per cell as well as the average TCR intensity accumulated at an interface relative to the total TCR signal (mEGFP) in the cell (n=8 contacts analyzed).

(**C and D**) The same experiment was performed for TCR-$CD3^{FL}$ M12 cells interacting with MCC:I-E^{k+} APCs ($58\alpha^{-}\beta^{-}$). (**C**) Long arrows indicate TCR accumulation that was scored as a contact, while short arrows indicate small TCR accumulations at the cell-cell interface that were not scored as contacts but were frequently observed. (**D**) The number of scored contacts are shown as in above (n=83) with insets indicating TCR accumulation for n=10 contacts.

(**E and F**) The same experiment was performed for (**E**) TCR-$CD3^{FL}$ $58\alpha^{-}\beta^{-}$ cells interacting with MCC:I-E^{k+} APCs (M12) and (**F**) scored (n=45 cells) as above with TCR accumulation for n=9 contacts.

Movie S1. Donor recovery after acceptor photobleaching in $CD3^T$-only cells, related to figure 3A.
$CD3^T$ -only cells adhered to a glass coverslip in HBSS+2% FCS were imaged by TIRFM. Movie is at 20 frames per second. Left image is mEGFP (donor) in grey scale, middle image is mCherry (acceptor) in grey scale, and right image is mEGFP in pseudo color. Intensities are set as in **Figure 3A**. Best viewed with video looped.

Movie S2. Donor recovery after acceptor photobleaching in TCR-$CD3^T$ cells, related to figure 3A.
TCR-$CD3^T$ cells were adhered to a glass coverslip in HBSS+2% FCS and imaged by TIRFM. Movie is at 20 frames per second. Left image is mEGFP (donor) in grey scale, middle image is mCherry (acceptor) in grey scale, and right image is mEGFP in pseudo color. Intensities are set as in **Figure 3A**. Best viewed with video looped.

Movie S3. TCR-$CD3^T$ cells accumulate TCR at contact interface with agonist pMHC+ APCs, related to Figure 6A bottom.
TCR-$CD3^T$ expressing M12 cells, expressing a TCRβ-mEGFP fusion (Kuhns et al., 2010), were co-cultured with MCC-IE^{k+} $58\alpha^-\beta^-$ APCs in a coverslip chamber slide in HBSS+2% FCS. DIC and mEGFP were collected every 30 seconds for 10-15 minutes to observe interactions. Movie is at 16 frames per second. Left image is DIC only, middle image is mEGFP, and right image is DIC+mEGFP overlay. Best viewed with video looped.

Movie S4. TCR-$CD3^T$ cells do not accumulate TCR at contact interface with control APCs, related to Figure 6A top.
TCR-$CD3^T$ expressing M12 cells, expressing a TCRβ-mEGFP fusion (Kuhns et al., 2010), were co-cultured with control parental $58\alpha^-\beta^-$ APCs (MCC-IE^{k+} negative) in a coverslip chamber slide in HBSS+2% FCS. DIC and mEGFP were collected every 30 seconds for 10-15 minutes to observe interactions. Movie is at 16 frames per second. Left image is DIC only, middle image is mEGFP, and right image is DIC+mEGFP overlay. Best viewed with video looped.

SUPPLEMENTAL EXPERIMENTAL PROCEDURES

Constructs

All expression constructs were built using the MSCV-based retroviral plasmids pP2 (IRES-puromycin resistance) and pZ4 (IRES-zeocin resistance) (Kuhns and Davis, 2007; Kuhns et al., 2010). The proteins encoded by the constructs used in this study are described by amino acid (aa) number beginning at the start methionine.

The constructs common to two or more assay systems include the following. pZ4-2B4α and pP2-2B4β-LmEGFP (used for ID-PRIME and EPOR but not FRET) were previously described (Kuhns and Davis, 2007; Kuhns et al., 2010). Here, a long flexible linker was used to space the mEGFP away from the TCR (AAAGGGGSGGGGSGGGGS). pP2-CD3T3 was generated by modifying pP2-CD3T2 (encoding CD3γ^T, δ^T, ε^T, and ζ^T with a C-terminal EE affinity tag (Kuhns et al., 2010)) to encode a truncated CD3ζ^T (aa: 1-57) lacking a C-terminal EE affinity tag. All polycistronic constructs were built following the strategies of Vignali and colleagues (Holst et al., 2008).

The constructs unique to the CD3ζζ ID-PRIME experiments were generated as follows. pP2-3T3 was modified (pP2-3T3ζ^T LAP1) to encode a linker (AAAGSGGSG) between residue 57 of CD3ζ^T and the LAP1 sequence. pP2-CD3FL-ζ^T LAP1 was similarly constructed but encoded the full-length CD3γ, δ, and ε subunits. A short GT linker was then encoded between LAP1 and a c-terminal myc tag prior to the stop codons. For CD3ζ^{LplA}, a unique construct was built (pP2 CD3ζ^T5hLplA^{W37V}) that encodes CD3ζ^T with a linker (GGGSAAA) between residue 57 of CD3ζ^T and hLplA^{W37V}. Finally, a short linker (GTGG) preceded the c-terminal HA tag. This was used in experiments with CD3^T-only and TCR-CD3^T cells. A second version was built that removed the LplA ATG between CD3ζ^T and hLplA^{W37V} since this was serving as a translation initiation site for free LplA. This version was used to generate CD3^{FL}-only and TCR-CD3^{FL} cells.

The constructs unique to the control FRET experiments are outlined below. pZ4-αTM encoding the extracellular domain of 2B4α fused to the transmembrane domain of EPOR and pP2-βTM encoding the extracellular domain of 2B4β fused to the transmembrane domain of EPOR were previously described (Kuhns et al., 2010). For control FRET experiments, pZ4-αTM was modified to generate constructs encoding the TCRα chimera fused to mCherry (mCh) via a short linker (AAAG; pZ4-αTM.mCh). Likewise, pP2-βTM was fused to mEGFP via a short linker (AAAG; pP2-βTM.mG). pP2-CD4-LmG encodes C-terminally truncated mouse CD4 (aa: 1-427) fused to mEGFP.

The constructs unique to the CD3ζζ FRET experiments are outlined below. pZ4-CD3ζTmCh and pP2-CD3ζTmG encode truncated CD3ζ (aa: 1-52) fused to mCherry or mEGFP, respectively, via a short GSAAA linker. Bi-cistronic constructs were also generated using a T2A cleavage peptide to link expression of the FRET pairs and the TCR subunits. pP2-CD3ζTmG.T2A.β encodes CD3ζ(aa:1-52)-GSAAA-mEGFP-GSG-T2A-2B4β, and pZ4-CD3ζTmCh.T2A.TCRα encodes CD3ζ(aa:1-52)-GSAAA-mCh-GSG-T2A-2B4α. pP2-CD3T3ζ^{Ng} was generated to encode CD3δ^T(aa: 1-132)-GSG-F2A-CD3γ^T(aa: 1-143)-RSGG-

T2A-CD3ε^{T}(aa: 1-139)-stop in order to express truncated CD3γ^{T}, δ^{T}, and ε^{T} off of a single plasmid without CD3ζ. pP2-CD3FLζ^{Ng} was generated with full length CD3 subunits in a similar manner.

The constructs unique to the EPOR system are outlined below. The pP2-CD3T3ζ^{E} construct was generated by replacing the gene segment encoding truncated CD3ζ with one encoding the CD3ζ-EPOR chimera composed of the CDζ extracellular and transmembrane domains (aa:1-51) fused to the juxtamembrane and intracellular domains (aa:273-508) of the human EPOR protein. pP2-CD3FLζ^{E} was generated with full length CD3 subunits in a similar manner.

Soluble class II pMHC were generated using modified baculovirus expression vectors, based on pAcGP67A (Pharmingen), encoding acidic or basic leucine zippers (generous gift of K.C. Garcia) according to the approach of Teyton and colleagues (Scott et al., 1996). The full extracellular domain of I-E^{k} alpha (aa: 26-216) was expressed as a fusion with the acidic leucine zipper, a BirA acceptor peptide, and a 6X his tag. The full I-E^{k} beta extracellular domain (31-225) was expressed as a fusion with the mouse hemoglobin d allele peptide (Hb 64-76) or moth cytochrome c (MCC 88-103) peptide at the N-terminus, via a short linker similarly to Kappler and colleagues (Crawford et al., 1998), and at the C-terminus with the basic leucine zipper and a 6X his tag. Purification was performed first with Ni-NTA affinity resin (Qiagen). Monomeric pMHC was then purified via a sizing column using an S200 (GE) via FPLC. For expression of MCC-IE^{k} and T102S-IE^{k} in 58$\alpha^{-}\beta^{-}$ or M12 cells, full length versions (ECD, TMD, and ICD) of the alpha and beta chains were cloned in frame with the TCR β leader sequence in pZ4 and pP2, respectively.

pMHC expression and purification

Baculovirus stocks were made in Sf9 cells and large-scale protein production was performed in Hi5 cells as previously described (Dukkipati et al., 2006). pMHC complexes were purified from media by affinity chromatography using a Nickel column (Qiagen) followed by biotinylation with BirA (Avidity), and size exclusion chromatography with a Superdex-200 column (GE Healthcare Life Sciences).

Cell lines

Ba/F3, M12 and 58$\alpha^{-}\beta^{-}$ cell lines were generated and analyzed by flow cytometry as previously described for TCR-CD3 expression and complex architecture via mAb mapping (not shown) (Ghendler et al., 1998; Kuhns and Davis, 2007; Kuhns et al., 2010). In brief, for each construct expressed in a cell line 1.3X10^{6} Phoenix E packaging cells were plated in complete DMEM (10% FCS) and cultured overnight at 37ºC in a 6 cm plate (Falcon). The media was exchanged and the cells were transfected with 1μg of the desired retroviral construct using Turbofect (Fermentas) according to the manufacturer's instructions. The media was changed after 24 hrs and the cells were shifted to 32ºC. The viral supernatant was then harvested at 48 and 72hrs. The supernantant for all constructs used to generate a cell line (**Fig. S2 G-I**) were then pooled and concentrated to 250μl using an Amicon Ultra 15 100kDa (Millipore). 1X10^{6} parental Ba/F3, M12 or 58$\alpha^{-}\beta^{-}$ cell were then plated in 2ml of complete RPMI in one well of a 12 well plate in 4μg/ml polybrene plus the viral supernatant and spun for 2hrs at 32ºC at 2700 rpm in a Legend XTR centrifuge (ThermoFisher). The media was exchanged immediately after spin infection and

the cells were cultured overnight at 37ºC prior to selection with 10μg/ml puromycin (LifeTech) and 100μg/ml Zeocin (LifeTech) splitting as necessary to keep thin and under heavy selection.

The constructs used to generate CD3-only and TCR-CD3 cell lines for ID-PRIME, FRET, and EPOR systems are illustrated in **Fig S2 G-I**. In each case, the matched CD3-only and TCR-CD3 lines were generated with the viral supernatant from the same number of constructs providing the same drug resistance. This was done to equalize viral competition for integration into a finite host genomic space, since we have observed that the number of constructs transduced into cells impacts the overall expression levels of any given gene regardless of the insert. To this end, the CD3-only ID-PRIME and EPOR cells were transduced with constructs encoding the ectodomains of TCRα and TCRβ fused to the TMD of EPOR (αTM and βTM, respectively) to fill the space occupied by the constructs encoding full length TCRα and TCRβ in the TCR-CD3 cells. The TMD of EPOR lacks the key TCRα and TCRβ TMD charge residues that are essential for complex assembly so the complex could not assemble in these cells and CD3ζζ could not associate with αTM (Call et al., 2002; Kuhns et al., 2010; Tan et al., 1991). For the FRET system, $CD3\zeta^{Ch}$ and $CD3\zeta^{G}$ were expressed independently in the CD3-only cells, or off of bicistronic constructs using the T2A cleavage peptide as described by Vignali and colleagues (Holst et al., 2008). For the ID-PRIME and FRET systems, two constructs (meaning two copies) of genes encoding CD3γ, CD3δ, and CD3ε were introduced into the cells relative to the single copy of each CD3ζ chimera.

Flow Cytometry

Anti-TCRβ mAb H57-597 BV421 (BioLegend), Anti-CD3ε mAb 2C11 PE-Cy7 (BioLegend), anti-CD3ε mAb 2C11 APC-eFluor 780 (eBiosciences), anti-Vα11 mAb RR8-1 APC (eBiosciences) and anti-class II MHC I-E^k mAb 14.4.4 FITC (BD) were used as indicated in the supplementary figure legends. The 2B4 TCR was used in this study. It is specific for MCC 88-103 presented in the class II MHC I-E^k (MCC-E^k). Hb 64-76 presented in I-E^k (Hb-E^k) was used as a null ligand. All cell lines were maintained at a density below $1X10^6$/ml and split the night before experiments to be in mid growth phase the day of the experiment.

EPOR assay

Ba/F3 proliferation experiments were performed and analyzed with one-way analysis of variance and Tukey's post-test for multiple comparisons similarly to our previous description (Kuhns et al., 2010). In brief, $2.5X10^4$ cells were setup in 96 well plates in triplicate under drug selection for a 3-day proliferation assay in the absence of IL-3 as a growth factor. Cells were enumerated by flow cytometry with count beads, which allowed the total cell number per well to be extrapolated.

ID-PRIME

ID-PRIME procedures were adapted from published protocols (Uttamapinant et al., 2013). $3x10^6$ CD3-only and TCR-CD3 M12 cells were loaded in serum free media with 100μM (in early experiments) and 50μM (in later experiments) of membrane permeant pAz (pAz-acetoxymethyl ester (AM)) for 45 minutes at 4ºC to minimize ligase activity. Cells were resuspended in pre-warmed HBSS+2% FCS and incubated at 37ºC to initiate ID-PRIME. Ligase activity was terminated with a large volume of ice-cold wash buffer (HBS) containing 40μM Lipoic Acid to competitively inhibit the enzyme. Cells were lysed in 1% n-Dodecyl-β-D-Maltopyranoside

(DDM, Anatrace). For TCR engagement experiments, $1.5x10^7$ APCs were pelleted with the TCR-CD3 cells at 4ºC after loading with pAz-4AM. The pellet was overlaid with pre-warmed HBSS+2% FCS and incubated in a water bath at 37ºC without pellet disruption to initiate the reaction. The samples were treated the same as above thereafter. For steady state analysis of the $CD3^{FL}$-only cells in comparison with the TCR-$CD3^{FL}$ cells, both were co-cultured with negative control APCs so that fold changes were more directly relatable to TCR-$CD3^{FL}$ cells with pMHC positive APCs. The $CD3^{T}$-only steady state comparisons to TCR-$CD3^{T}$ cells were done in the absence of APCs. Myc tagged CD3ζζ species were immunoprecipitated with EZ view anti-myc beads (Sigma). CuAAC was performed on anti-myc beads after overnight immunoprecipitation in a final 30µl volume with 167µM $CuSO_4$ (Sigma), 830µM BTTAA, 1.67µM Na Ascorbate (Sigma), 83µM TEMPOL (Sigma), and 16.7µM BALK for 30 minutes at room temp. The samples were separated by non-reducing SDS-PAGE before transferring to Immobilon FL (Millipore) and the blots were probed with anti-myc antibodies (mAb 9B11, Cell Signaling) followed by goat anti-mouse 2º antibodies DyLight 800 (Pierce) and streptavidin (SA) Alexa Fluor 680 (Invitrogen).

Blot Scanning and Analysis

Blots were scanned with an Odyssey two-laser (685nm and 785nm) infrared imaging system (LI-COR). Band intensities were quantitated after background subtraction with Image Studio Lite (LI-COR) software. The same scan intensities and area defined for background subtraction was used to quantitate $CD3\zeta^{LplA}\zeta^{LAP1}$ and $CD3\zeta^{LAP1}\zeta^{LAP1}$ bands in both the SA and myc channels for comparison within individual experiments. Values for SA signals were normalized to the CD3-only or control APC $CD3\zeta^{LplA}\zeta^{LAP1}$ signal for statistical comparison between experiments to account for blot-to-blot variations in signaling intensity. Figure images were also generated with Image Studio Lite (LI-COR). For all figures gamma = 1. In main figures, minimum background SA levels were set to subtract background and render sharp bands for the cis $CD3\zeta^{LplA}\zeta^{LAP1}$ modules since these species were the focus of the hypothesis being tested. For example, in **Figure 1D** the minimum signal is set at 221 (scan intensity = 5). At these settings, the weak SA $CD3\zeta^{LplA}\zeta^{LAP1}$ modules were not visible.

Peptide-MHC Surfaces

Biotinylated poly-L-lysine coated coverslips were incubated with 10µg/ml streptavidin, washed, and incubated with solutions containing 10µg/ml pMHC (Hb:I-E^k or MCC:I-E^k) and 1µg/ml anti-H2-D^d antibody similarly to Huse, Klein, et al. (Huse et al., 2007). For MCC-E^k (agonist) dilution experiments into Hb-E^k (null), the total pMHC concentrations used for coating the plate were kept constant at 10µg/ml. M12 cells expressing TCR-CD3 complexes with CD3ζ FRET probe chimeras were cultured on the pMHC surfaces for 30 minutes at 37ºC prior to imaging.

Microscopy

All live cell wide field and TIRF imaging was performed at 37ºC, 5% CO_2, and 50% relative humidity. Live cell three-channel sensitized emission wide field and TIRF imaging was acquired with an Olympus IX81 fluorescent microscope using a 60X APON TIRF objective (NA 1.49) coupled to a CellTIRF illuminator. A Lambda XL (Sutter Instruments) was used for wide field imaging. TIRFM was performed with a 20mW 561nm diode laser (Melles Griot) and the 488nm line of a 50mW multi-line argon laser (Melles Griot) separated with an acousto-optical tunable filter (AOTF; Laser Launch, LLC). The power output for the 488nm line was adjusted to match

that of the 561nm line through the objective. All images were collected with 100 millisecond exposures (Hamamatsu Photonics Image EM EMCCD; zero intensification; 1 pixel = 0.27µm (H) x 0.27µm (V) at 60x). TIRF imaging of donor recovery after acceptor photobleaching was performed with a Marianas microscopy workstation built on a Zeiss Axio Observer Z1 (Intelligent Imaging Innovations, Inc. (3I)) using a Zeiss 63X Alpha Plan-Apochromatic TIRF objective (NA 1.46) coupled to a Zeiss TIRF slider. Illumination was performed with a Laser Stack (3I) containing 50mW 488nm and 561nm solid-state lasers set at 20% power output. Photo ablation of mCherry was performed with a Vector high-speed point scanner (3I) at 20% 561nm laser output within a 25.8µm^2 region of interest (412 pixels) over the course of 5.7 seconds. All images were collected with 100-millisecond exposure at 500 millisecond intervals (Photometrics Evolve EMCCD; 100 intensification; 1 pixel = 0.25µm (H) x 0.25µm (V) at 63x).

Wide field live cell imaging for cell-cell interactions was performed with the Marianas system under environment control using a Sutter DG-4 for illumination. DIC (10 milliseconds, intensification = 1) and mEGFP (5 milliseconds, intensification = 170) images were collected every 30 seconds for 10-15 minutes for time-lapse experiments with a Zeiss 40x EC Plan-Neofluar objective (NA 1.3). pMHC$^+$ APCs and TCR-CD3 cells were co-pelleted at 5:1 and cultured for 5 minutes at 37ºC in a water bath to enumerate contacts. The cell pellet was gently disrupted and transferred to an eight-chamber coverslip (LabTek) in HBSS + 2% FCS. A mid-plane DIC image and thirty 1µm focal steps were collected for mEGFP to assess all contacts on the sphere of a TCR-CD3 cell using a Zeiss 63X Alpha Plan-Apochromatic TIRF objective (NA 1.46).

Image Analysis

FRETc was analyzed using SlideBook 5 software (3I) according to Youvan, et al. (**Figure S5A**)(Youvan et al., 1997). Cells expressing single fluorophore tags were used to calculate spectral bleed-through coefficients for each experiment. nFRETc values represent the mean FRETc values divided by the mean mEGFP for a single cell (Vanderklish et al., 2000). For analysis of TIRF images, background intensity in the mCherry channel from 20 individual fields across 8 experiments was determined to be 1809+/-35 (sdev). Cells with mCherry intensity at or above 2500 were considered for data analysis to ensure cell membranes were in close opposition to the surface for illumination by the TIRF evanescent wave. Subset analysis for FRETc was performed for cells with the values within the shaded gates (**Figure 2 and 5**). Note that we commonly observe mCherry accumulating in puncta more than mEGFP. All representative images are background subtracted.

$FRET_E$ analysis was performed using SlideBook 6 software (3I). The median intensity for mEGFP and mCherry were extracted from the region of interest (25.8µm^2 ROI; 412 pixels) targeted for mCherry ablation. Background subtracted mEGFP values for the time points immediately before and after photobleaching were used to calculate $FRET_E = 1- (Q/DQ)$ where Q equals quenched and DQ equals dequenched fluorescence of the mEGFP as previously reported (Xu et al., 2008). For all $FRET_E$ experiments, cells were selected for subset analysis based on the background subtracted pre-bleach intensity of mEGFP and mCherry if they fell within an mEGFP:mCherry ratio ranging from 0.5 to 1.5 and had mCherry post-bleach levels below 20% of pre-bleach levels (we average 90% ablation) using MATLAB software (MathWorks) (**Figure S6E** and not shown). The pre-bleach expression range from center was

chosen considering a number of variables, including a lower intensity of mEGFP for molecules transferring energy to a mCherry, the relative 'brightness' of mEGFP being greater than mCherry, and that the perceived brightness of a fluorescent protein is dependent on several highly variable factors (Shaner et al., 2005). In all experiments the results for the total population and subsets were concordant, indicating that the differences observed were reflective of the population at large.

The number of cell-cell contacts between TCR-CD3 cells and $pMHC^{+}$ APCs were estimated by enumerating the total number of $TCR\beta\text{-}mEGFP^{+}$ cells and scoring for accumulation of mEGFP at the interface with a $mEGFP^{-}$ cell APC. Accumulation of mEGFP was estimated by setting a mask including the fluorescence for a whole mEGFP positive cell and determining both the mean and total fluorescence within the cell. A separate mask was then set for the contact interface using the mean from the total cell as the minimum mask value. The total fluorescence intensity at the contact area was then compared relative to the total intensity of the cell to determine the percent mEGFP localized to the contact interface.

Statistical Analysis

All statistical analysis indicated in the Figure Legends were performed with Prism 5.0 (GraphPad Software, Inc). For the EPOR experiments, One-Way Analysis of Variance (ANOVA) was performed with a Tukey's post test for multiple comparisons. The ID-PRIME and imaging experiments involved normalized data or non-normally distributed cell populations. Therefore, the Mann-Whitney t test and Kruskal-Wallis ANOVA with a Dunn's multiple comparisons post-test were performed where appropriate.

SUPPLEMENTAL REFERENCES

Bonifacino, J.S., Suzuki, C.K., Lippincott-Schwartz, J., Weissman, A.M., and Klausner, R.D. (1989). Pre-Golgi degradation of newly synthesized T-cell antigen receptor chains: intrinsic sensitivity and the role of subunit assembly. J Cell Biol *109*, 73-83.

Crawford, F., Kozono, H., White, J., Marrack, P., and Kappler, J. (1998). Detection of antigen-specific T cells with multivalent soluble class II MHC covalent peptide complexes. Immunity *8*, 675-682.

Dukkipati, A., Vaclavikova, J., Waghray, D., and Garcia, K.C. (2006). In vitro reconstitution and preparative purification of complexes between the chemokine receptor CXCR4 and its ligands SDF-1alpha, gp120-CD4 and AMD3100. Protein Expr Purif *50*, 203-214.

Ghendler, Y., Smolyar, A., Chang, H.C., and Reinherz, E.L. (1998). One of the CD3epsilon subunits within a T cell receptor complex lies in close proximity to the Cbeta FG loop. J Exp Med *187*, 1529-1536.

Holst, J., Wang, H., Eder, K.D., Workman, C.J., Boyd, K.L., Baquet, Z., Singh, H., Forbes, K., Chruscinski, A., Smeyne, R.*, et al.* (2008). Scalable signaling mediated by T cell antigen receptor-CD3 ITAMs ensures effective negative selection and prevents autoimmunity. Nat Immunol *9*, 658-666.

Huse, M., Klein, L.O., Girvin, A.T., Faraj, J.M., Li, Q.J., Kuhns, M.S., and Davis, M.M. (2007). Spatial and temporal dynamics of T cell receptor signaling with a photoactivatable agonist. Immunity *27*, 76-88.

Scott, C.A., Garcia, K.C., Carbone, F.R., Wilson, I.A., and Teyton, L. (1996). Role of chain pairing for the production of functional soluble IA major histocompatibility complex class II molecules. The Journal of experimental medicine *183*, 2087-2095.

Shaner, N.C., Steinbach, P.A., and Tsien, R.Y. (2005). A guide to choosing fluorescent proteins. Nat Methods *2*, 905-909.

Tan, L., Turner, J., and Weiss, A. (1991). Regions of the T cell receptor alpha and beta chains that are responsible for interactions with CD3. Journal of Experimental Medicine *173*, 1247-1256.